ELSEVIER

PII: S0032-3861(97)00313-3

Polymer Vol. 39 No. 3, pp. 533–545, 1998
© 1997 Elsevier Science Ltd
Printed in Great Britain. All rights reserved
0032-3861/97/$17.00+0.00

Morphology, thermomechanical and barrier properties of polypropylene-ethylene vinyl alcohol blends

J.B. Faisant[†,a], A. Aït-Kadi[a,*], M. Bousmina[a] and L. Deschênes[b]
[a]*Chemical Engineering Department and CERSIM Laval University, Pavilion Pouliot, Quebec (QC), Canada G1K 7P4*
[b]*Food Research and Development Centre, 3600, Casavant Boulevard West, St Hyacinthe (QC), Canada J2S 8E3*
(Received 29 May 1996; revised 13 March 1997)

Processing as well as physical properties of polypropylene (PP)/ethylene vinyl alcohol (EVOH) and PP/EVOH/high density polyethylene (HDPE) blends have been investigated. Blends were prepared both on a batch mixer and a twin-screw extruder. Extrusion was followed by drawing between two roll mills. Minor phase deformation during stretching was analysed using shape relaxation theory. When PP/EVOH blends were prepared on the internal mixer, low aspect ratio EVOH particles were obtained. This did not lead to appreciable barrier properties improvement. In contrast, an EVOH fibrillar and lamellar morphology obtained by extrusion and drawing was found to induce a significant decrease (85%) in O_2 permeability for only 20 vol.% EVOH content. The barrier properties of the PP/EVOH extruded blends were predicted using a hybrid diffusion model that takes into account the morphology of the blends. When PP.g.Maleic-Anhydride is added to PP/EVOH blends and for high draw ratios, elongation at break remains important, even at 20 vol.% EVOH. This result, together with the large gain in barrier properties, makes the PP/PP.g.MA-EVOH blends a proper material for applications such as food packaging. The use of HDPE/EVOH blend with PP intended to keep the EVOH well dispersed in the system did not give the expected barrier properties, due to the poor adhesion at the PP–HDPE interface. © 1997 Elsevier Science Ltd.

(Keywords: polypropylene; polyethylene; ethylene vinyl alcohol)

INTRODUCTION

It is a difficult task to design a low-cost material for packaging or gasoline tanks that meets technical requirements such as barrier and mechanical properties. These materials have to be easy to process at low cost and also have to be recyclable[1]. Optical clarity is another property which is often required, especially in the case of food packaging. Plastic containers with high barrier properties are usually multi-layers materials produced by coextrusion[2–7]. This is a complex and expensive technology and the final product is not recyclable. Polymer blending appears to be a more beneficial alternative in designing materials with enhanced physical properties with the possibility of recycling the final product[8–11]. Addition of a small quantity of a barrier material into a low-cost matrix material can lead to a low-cost product with greatly improved barrier properties[12–21].

Polypropylene (PP) is a commodity polymer with good mechanical and good barrier properties to H_2O. This could be a useful polymer for food containers manufacturing, but its poor barrier properties to O_2 limits applications[21]. On the other hand, EVOH, a copolymer of ethylene and vinyl alcohol, has high barrier properties to gases such as O_2 and CO_2 and has high resistance to hydrocarbons. This makes it an interesting candidate for food applications. However, its cost is higher[22]: 2.5–3 US$ lb^{-1} as compared to 0.4–0.7 US$ lb^{-1} for a blow molding PP grade[23,24] (prices: October 1994–March 1995). EVOH is also highly sensitive to humidity which alters its resistance to oxygen permeation[25,26]. This is one of the reasons why so many studies have been concerned with combining PP or polyethylene (PE) with EVOH in a multi-layers structure by coextrusion[1,2,6,7]. Another alternative is to disperse EVOH into a PP matrix. By optimizing the EVOH particle's morphology, one can obtain a low-cost material with high barrier properties. Using such a strategy, Lohfink and Kamal[15] and Kamal *et al.*[16,17] reduced by 60% the permeability of PP to O_2 by adding 25 vol.% EVOH. However, they had to incorporate a slit die into the extrusion process. This technology is not easy to transfer to usual packaging processes such as blow molding or injection molding. No report was given of PP/EVOH blends mechanical properties such as Young modulus, yield stress or elongation at break. Gopalakrishnan *et al.*[19] and Kit *et al.*[20] used Kamal's[16,17] approach to enhance O_2 properties of polyethyleneterephtalate (PET) and polyethylene 2,6 naphtalate (PEN). Blending PET with EVOH with and without compatibilizer resulted in a maximum increase of 80% in barrier properties for 20 wt% EVOH. Blending PEN with EVOH lead to a 65% increase in barrier properties for 15 wt% EVOH. In contrast, Gaylord *et al.*[18] added polyvinyl alcohol (PVAI: a high barrier properties polymer) to PE by melt-blending. This did not improve the barrier properties, probably due to water absorption by PVAL.

* To whom correspondence should be addressed
† This paper is dedicated to the memory of the co-author who died on 27 November, 1996

The principal objectives of this work are: (i) to significantly increase the barrier properties to O_2 for PP/EVOH blends in comparison to previous works; the blending process must be easy to transfer to packaging industry; (ii) to keep the highest possible mechanical properties when blending PP with EVOH; (iii) to study the influence of processing conditions on the properties of the blends; (iv) to study the effect of a third compound (e.g. a compatibilizer or high density polyethylene) on mechanical and barrier properties of PP/EVOH blends; (v) to quantitatively analyse diffusion of gas through blends with various morphologies.

EXPERIMENTAL

Multi-layers structures are known to give the highest barrier properties. We therefore prepared multi-layers PP/EVOH films to estimate the maximum barrier properties for a given EVOH concentration. Two blending processes were chosen to increase barrier properties of the pure PP. Both processes can be transposed to larger scale industrial blending processes. A series of PP/EVOH blends were prepared on a batch mixer to estimate the permeability to O_2 of dispersion type systems. Blends were hot pressed after batch mixing. Other blends were prepared by extrusion, namely PP/EVOH, PP/PP.g.MA/EVOH and PP/HDPE-EVOH. The HDPE phase is aimed at keeping the EVOH particles well dispersed in the final product as will be explained in the blends morphology section. Extruded films were drawn to obtain an elongated structure suitable for enhanced barrier properties. Rheological properties of pure polymers were analysed. Mechanical, thermal and permeability measurements were performed on both pure polymers and blends. Blends morphology was also studied.

Materials

Three grades of PP have been chosen: a PP with a high melt viscosity (will be referred to as PPhv: melt flow index (MFI) of 0.3°C min^{-1} at 230°C under 2.15 kg[24]) and a PP with a lower melt viscosity (will be referred to as PPlv: MFI = 2°C min^{-1} [24]). They were provided by Himont, Canada. The PPhv is a profax 613-D resin while the PPlv is a profax 256-M resin. Both are transparent grades meeting the Food and Drug Administration (FDA) requirements. Since PP and EVOH are incompatible, a PP resin grafted with maleic anhydride was chosen as a compatibilizer (referred to as PP.g.MA). This is a MODIC-P30OF resin provided by Mitsubishi Chemical Co., Japan.

A high density polyethylene (HDPE) was also used since it was believed to be compatible with EVOH through ethylene groups. It is a Novapol HB-L455 A/S grade (MFI = 0.4 °C min^{-1} at 190°C under 2.15 kg[27]) provided by Novacor–Canada. This resin also meets FDA requirements[27].

The EVOH copolymer was provided by EVAL-CO of America. It is a F101 resin containing 32% moles of ethylene, with good optical clarity and FDA approved[22].

Blends preparation

Blends were prepared either using a Haake Büchler twin roller-blades batch mixer or a Haake Büchler twin screw corotating extruder. Since the recommended processing temperature for EVOH ranges from 200 to 240°C[22] and the recommended processing temperature for PPhv, PPlv and PP.g.MA ranges from 190 to 230°C[24], a processing temperature of 200–230°C was chosen for blending EVOH to PP. The recommended processing temperature for HDPE ranges from 160 to 205°C. A 200°C temperature was therefore chosen for blending HDPE and EVOH to PP. Processing conditions are summarized on *Table 1*. Draw ratios are given for extruded and drawn films.

To better understand the relationships between morphology and barrier properties of the blends prepared by extrusion and stretching, two types of extreme morphological situations were designed for comparison purposes. They are explained in the following two sections.

Multi-layers films. For comparison purposes, films of PPlv and EVOH of thicknesses 42 and 8 μm, respectively, were prepared by hot pressing and then assembled in a PPlv/EVOH/PPlv sandwich-like structure and hot pressed at 205°C, under 20 MPa for 90 s.

Table 1 Processing conditions on the batch mixer

Material		Processing	T = 200°C 30 rpm	38 rpm	60 rpm	T = 230°C 38 rpm	60 rpm	Draw ratio
PP1v/EVOH	88/12 vol.%	Batch mixer	X		X			
	75/25 vol.%		X		X			
	65/35 vol.%		X					
	55/45 vol.%		X					
	45/55 vol.%		X					
	35/65 vol.%		X					
PPhv/EVOH	88/12 vol.%			X	X	X	X	
	75/25 vol.%			X	X	X	X	
PP1v/EVOH	90/100 vol.%	One-step extrusion	X					1–10
	80/20 vol.%		X					1–10
PPhv/EVOH	90/10 vol.%		X					1–3
PP1v/PP.g.MA/EVOH	80/10/10 vol.%	Two-step extrusion	X					1–10
PP1v/(PP.g.MA-EVOH)	80/(10-10) vol.%		X					1–10
	60/(20-20) vol.%		X					1–10
PPhv/(PP1v-EVOH)	80/(10-10) vol.%		X					1–3
PP1v/(HDPE-EVOH)	60/(20-20) vol.%		X					1–10
	50/(30-20) vol.%		X					1–10

Table 2 Viscosity ratios η_{EVOH}/η_{PP} obtained from small amplitude oscillatory shear measurements

ω (rad s^{-1})	η_{EVOH}/η_{PP} at 200°C			η_{EVOH}/η_{PP} at 230°C
	PPlv	PPhv	PP.g.MA	PP.g.MA
30	1.087	0.586	0.716	0.840
100	1.454	0.890	0.972	1.041
200	1.721	1.134	1.160	1.179

first-step mixture. Different PPlv/EVOH compositions were tried to produce an interpenetrated PP/EVOH network. 75/25–35/65 vol.% by steps of 10 vol.%. In all cases, scanning electron microscopy (SEM) did not give evidence of an interpenetrated network (see the later section on morphology). The composition PPlv/EVOH 50/50 vol.% was selected.

- Another strategy consists of mixing HDPE with EVOH in a first step to obtain an interpenetrated network. Two compositions HDPE/EVOH 50/50 and 60/40 in volume were selected. HDPE and EVOH are expected to be immiscible whereas HDPE is known to be immiscible with PP. One therefore expects that during the second step, when mixing HDPE/EVOH with polypropylene, HDPE will remain interpenetrated with EVOH.
- A further procedure for the first-step mixing was to mix a PP.g.MA to EVOH (50/50 vol.%). PP.g.MA adheres to EVOH due to chemical grafting between maleic anhydride groups and EVOH. It was believed that adhesion enhancement between PP and EVOH would decrease voids at the interface. This should therefore decrease the permeability and enhance mechanical properties.

Table 3 Materials properties

	PPhv	PPlv	PP.g.MA	HDPE	EVOH
Density (10^{-3} kg m^{-3})	0.90	0.90	0.90	0.95	1.19
Melting temperature (°C)	158	142	161	128	185
Crystallinity (%)	52	45	36	62	63
Tensile modulus (GPa)	0.69	0.57		1.20	2.90
Tensile strength at yield (MPa)	25.2	5.9		28.0	80.1
Elongation at break (%)	1	369	547	800	156

Batch blending. Due to the low viscosity of the PPlv grade and since the viscosity ratio η_{EVOH}/η_{PP} increases with temperature, we only selected the lower mixing temperature (200°C) for this grade to increase the possibility of stretching and breaking EVOH particles during mixing.

Some of the samples were hot pressed after mixing using a Carver Press at 180°C, increasing steadily the pressure from 0 to about 20 MPa for 60 s. Afterwards the sample was quenched by circulating cold water within the press plates. This procedure was designed to flatten the EVOH particles in the shape of platelets, to obtain optimal barrier properties.

Continuous blending. The EVOH concentrations chosen were 10 and 20 vol.%. The rotor speed (30 rpm) and the extrusion temperature (200°C) were chosen to minimize the viscosity ratio, η_{EVOH}/η_{PP}. This choice was based on the viscosity data obtained from small amplitude oscillatory shear measurements, using the Cox–Merz rule ($|\eta^*(\omega)| = \eta(\dot{\gamma})$ for $\omega = \dot{\gamma}$). This rule is known to hold for several homopolymers and polymer solutions. The viscosity ratios $\eta EVOH/\eta_{PP}$ given on *Table 2* have been calculated from dynamic rheometry data. A temperature of 200°C and a low extrusion speed of 30 rpm were chosen to ensure a low viscosity ratio η_{EVOH}/η_{PP}. After extrusion, samples were drawn between rolls at different draw ratios. The die width of the extruder was 50 mm and the flat die thickness has been set at a minimum value of 250 μm.

Blends were processed in one or two steps. In the one-step process, the different polymers were mixed at the same time and drawn as tapes. The two-steps mixing is an effective strategy to achieve high barrier properties. By choosing appropriate proportions of the compounds and processing conditions, one may obtain interpenetrating-type morphologies. If this interpenetrated polymer network is then mixed during a second step with the PP matrix, one may expect to produce the desired morphology for enhancing both mechanical and barrier properties.

Several processing conditions have been tested for the two-step mixing:

- In the first condition, EVOH has been mixed with the low viscosity PPlv during the first step at 50/50 vol.% composition. In the second step, the mixture was added to the high viscosity PPhv to facilitate deformability of the

For these three procedures, EVOH concentration in the final material was 10 or 20 vol.%. For the following sections, we adopt the following convention: when polymers P1, P2 and P3 are mixed in a single step, the blend is named P1/P2/P3. When polymers P1 and P2 are mixed in a first step, and polymer P3 added during a second step, the blend is named P3/(P1-P2).

Characterization

The characteristics of the pure components used in this study are listed in *Table 3*. Densities were given by the manufacturers. Melting point temperature and crystallinity were determined by differential scanning calorimetry. Mechanical properties were obtained using a drawing machine (see below).

Rheological measurements. Small oscillatory shear measurements were performed on a Rheometrics System 4 mechanical spectrometer in the parallel plate geometry. The specimens were molded at 200°C in the form of 25 mm diameter disks using a Carver Laboratory press. The oscillatory shear measurements were conducted at different temperatures ranging from 190 to 230°C. All the measurements were performed under nitrogen purge to avoid thermal degradation at high temperatures. No thermal degradation occurred during the tests as verified by 40 min time sweep tests. The frequency was varied from 0.05 to 100 rad s^{-1}. Depending on frequency and temperature, a small enough strain was set so that the rheological behaviour is in the linear viscoelastic zone.

Thermal behaviour. Melting temperatures, T_m, and heat of fusion, ΔH_m, were determined using a Perkin Elmer differential scanning calorimeter (d.s.c.-4) at a scanning rate of 10°C min^{-1}. Heat of fusion ΔH_m was calculated from the surface below the melting peak. The crystallinity, χ, of PP and EVOH phases were determined according to

$$\chi = \Delta H_m / \Delta H_0 \quad (1)$$

where ΔH_0 is the heat of fusion at 100% crystallinity. For PP, we took $\Delta H_0^{PP} = 153.0\ J\ g^{-1}$ as given by Mirabella[28]. Since EVOH contains 82 wt% of vinyl alcohol[22] and since $\Delta H_0^{PVAL} = 156.2\ J\ g^{-1}$ (see Hwang *et al.*[29]), we took for EVOH $\Delta H_0^{EVOH} = 0.82 \times \Delta H_0^{PVAL} = 128.1\ J\ g^{-1}$

Mechanical properties. Two types of mechanical tests were carried out: tensile tests and lap shear tests. Both tests were performed using an Instron tensile machine at room temperature and at a loading speed of 0.33 mm s^{-1}.

Tensile tests were performed to determine mechanical properties such as modulus, yield strength, stress and elongation at break. Samples were molded using a Carver Laboratory Press at a temperature approximately 20°C above the melting point of the matrix and were quenched with circulating cold water. The specimen dimensions were in accordance with ASTM-D638.

Lap shear tests were also conducted to evaluate the adhesion strength between EVOH and the different PP grades used in this work. Thin films of EVOH and PP (thickness = 0.8 mm) were molded at a temperature 20°C above their melting temperatures. Part of the surface of an EVOH film was then stuck to part of the surface of a PP film by hot pressing at 180°C under 15 MPa during 60 s. The samples were then cut and drawn on the Instron machine. The dimensions of the contact surface between PP and EVOH films were on average 10 mm along the draw direction and 20 mm along the direction transverse to the stretching.

For tensile tests as well as lap shear tests, a minimum of five samples were tested for each blend series and statistical average values as well as standard deviations were calculated.

Morphological analysis. The morphology of the blends was observed using a Jeol JSM-840A scanning electron microscope. Samples were prepared by cryofracture in liquid nitrogen. The cryofractured surfaces were coated with a gold/palladium mixture under vacuum to avoid charging.

Barriers properties. The permeabilities to oxygen were determined using a Mocon Ox-Tran 10/50A SATC permeability apparatus. This standard equipment has been fully described elsewhere[30]. In brief, this equipment has 20 permeation cells (permeation area: 50 cm^2) and uses a coulometric cell as an oxygen sensor. Permeation cells are divided in two chambers separated by the test material. Humid oxygen passed through the upper chamber. Humid carrier gas (99% nitrogen and 1% hydrogen) passed through the bottom chamber sweeping the permeant oxygen to the sensor. The temperature was controlled by a loop from a circulating thermostated water bath, placed on the top and the bottom of the permeability cells. External bubblers used to allow humid testing were placed in a thermostated bath at the same temperature as the permeation cells to avoid water condensation in the tubings. With this system, a relative humidity level of 95% was obtained in the measurement cells.

Running operation procedure described by Mocon[30] was applied. The surface of the samples was smaller than that of the cells. The samples were then masked with Mocon aluminium foils before testing. Depending on the size of our samples, aperture of the foils was varied from 75 to 600 mm^2.

RESULTS AND DISCUSSION

The results are divided into four parts. First, the thermal properties of the blends are presented. Second, we present results concerning the blends morphologies. Third, we discuss the mechanical properties with respect to the blend morphology. Finally, the results concerning permeabilities will be analysed and correlated to the phase morphologies.

Table 4 Thermal properties of PP/EVOH systems blended on the batch mixer

Sample		T_{mixing} (°)	Ω (rpm)	$T_{melting}$ of the polyolefin (°C)	PP or HDPE crystallinity (%)	$T_{melting}$ of EVOH (°C)	EVOH crystallinity (%)
PPhv		–	–	158	52		
PPlv		–	–	142	45		
HDPE		–	–	128	62		
EVOH		–	–			189	69
		200	30			185	62
		230	30			185	63
PPhv/EVOH	88/12 vol.%	200	38	163	49	185	25
	88/12 vol.%	230	38	162	47	182	45
	75/25 vol.%	200	38	162	55	184	30
	75/25 vol.%	200	60	162	50	184	15
	75/25 vol.%	200	38	161	57	183	17
PPlv/EVOH	88/12 vol.%	200	30	144	29	185	39
	75/25 vol.%	200	30	144	32	185	53
	88/12 vol.%	200	60	145	37	184	26
	75/25 vol.%	200	60	144	34	184	30
HDPE/EVOH	60/40 vol.%	200	30	128	59	184	66
	40/60 vol.%	200	30	128	60	184	70

Thermal properties

Melting point temperatures and crystallinity are presented in *Table 4*. These results concern PP/EVOH blends mixed on the batch mixer and HDPE/EVOH extruded blends.

Thermograms of PP/EVOH blends show two peaks, one corresponding to the melting of PP (from 120 to 165°C, T_m = 142°C for PPlv and 158°C for PPhv) and the other one to the melting of EVOH (from 155 to 190°C, T_m = 185°C). Due to low EVOH concentration, EVOH melting peaks for blends are rather small. Due to the overlap between melting zones of PPhv and EVOH, the area under the EVOH melting peak may be underestimated. Therefore, EVOH crystallinity may be underestimated for PPhv/EVOH blends.

No significant change in crystallinity after mixing is observed for PPhv. For pure EVOH, crystallinity decreased from 69% prior to mixing to approximately 63% after mixing. After mixing EVOH with PPhv or PPlv, our results show an important decrease in EVOH crystallinity. This decrease can be partly attributed to the underestimate of EVOH crystallinity in the case of PPhv/EVOH blends. This question will not be discussed here since no further analyses of these results were performed.

Thermograms of HDPE/EVOH blends show two peaks, one corresponding to the melting of HDPE (from 80 to 125°C, T_m = 128°C) and the other one to the melting of EVOH (from 155 to 190°C). Since there is no overlap between HDPE and EVOH melting peaks, uncertainty on crystallinity measurements are small. No significant decrease in crystallinity is observed for HDPE and EVOH after blending on the extruder.

Morphology

Batch blending. It has been shown[31,32] that a screw speed of N rpm on an internal mixer similar to the one used in this study is equivalent to a shear rate of approximately $N\ s^{-1}$. If the Cox–Merz rule holds for homopolymers, it is possible to use linear viscoelastic data to evaluate the viscosity ratio. Viscosity ratios given below were calculated at 30 rad s^{-1} from rheometry data.

Let us first discuss the behaviour of the blends containing less than 25 vol.% EVOH. For the high viscosity PP (PPhv: $\eta_{EVOH}/\eta_{PPhv} = 0.5$ at 200°C and 38 rpm), a coarse structure is observed with EVOH particles as large as 100 μm [see *Figure 1a*]. The poor mixing may be due to the deviation of the viscosity ratio from unity[33]. Gopalkrishnan *et al.*[19] pointed out that a good mixing of EVOH with PET is obtained for a viscosity ratio close to unity. Lohfink and Kamal[15] blended PP to EVOH with viscosity ratios even larger than 1. For low viscosity PP(PPlv: $\eta_{EVOH}/\eta_{PPlv} \approx 1$ at 200°C and 30 rpm), a finer structure is obtained [see *Figure 1b*].

In the case of PPlv/EVOH with compositions ranging from 25 to 65 vol.% EVOH, we did not observe any interpenetrated network similar to morphology. For PPlv/EVOH compositions ranging from 65/35 to 45/55, composite blends were obtained with small droplets included in larger particles.

Continuous blending. From the temperature profile of the extruded film under stretching, one can estimate if any large macromelecular orientation may be expected. Let us assume a radiative heat transfer from the hot polymer film to the surrounding air. The film density, ρ, and heat capacity

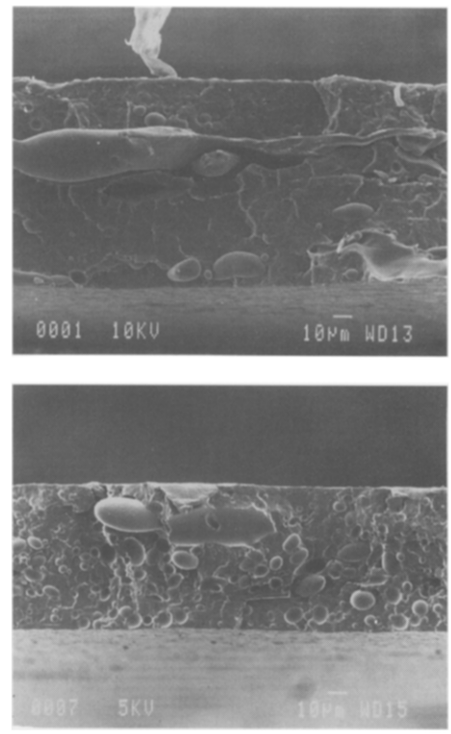

Figure 1 SEM micrograph for a PP/EVOH system blended on the batch mixer: (a) PPhv/EVOH 75/25 vol.% (T_{mix} = 200°C, 38 rpm); (b) PPlv/EVOH 75/25 vol.% (T_{mix} = 200°C, 30 rpm)

C_p are supposed to be constant from the die to the rolls. Under these conditions, the core temperature $T(x)$ of an extruded polymeric film at a position x from the die is given by[34]

$$\frac{T(x)-T_r}{T_0-T_r} = \exp\left(-\frac{x}{\rho e u C_p}\left(K\left(\frac{u}{x}\right)^{1/2}+h_r\right)\right) \quad (2)$$

where u is the extrusion speed of the film, e is the film thickness, K is a parameter depending on the physical properties of the ambient fluid (air in this case) at the temperature considered. As long as the film temperature varies only by a few tens of degree, K can be considered as a constant[34]. h_r is the radiative heat transfer coefficient, T_r is the room temperature (20°C) and T_0 is the temperature of the polymer in the die. For a polypropylene film extruded at 200°C, we obtain

$$T(x) = 180\exp\left(-10^{-6}\frac{x}{eu}\left(1.75\left(\frac{u}{x}\right)^{1/2}+4.91\right)\right)+20 \quad (3)$$

When the draw ratio is 1, there is no stretching of the film. Therefore, no decrease in the film width is observed between the die and the two rolls. The rolls speed is equal to the extrusion speed. Since the rolls speed can be varied and measured, it is therefore easy to estimate the extrusion speed. At 30 rpm, the extrusion speed is close to 0.01 m s^{-1} for the PP grades. The film polymer was drawn within the first 5 cm from the die. Depending on the draw ratio, the film thickness of PP films ranges from 0.2 to 1 mm. Film core temperature as a function of the distance from the die for different thicknesses are shown in *Figure 2*. At a distance of 5 cm, the temperature was 176°C for e = 0.2 mm, whereas

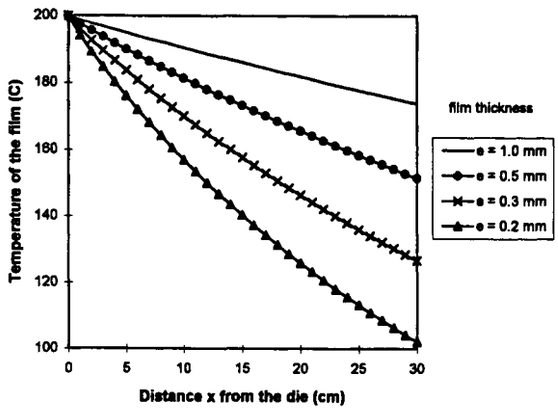

Figure 2 Film core temperature *versus* the distance x from the die for different thicknesses, e

for $e = 1$ mm the temperature was 196°C. In this temperature range, CP remains constant and density variations are small so that assumptions of constant heat capacity and density hold in this case. K can be considered a constant as well. This means that equation (2) is a good approximation for estimating the temperature profile of extruded films. For the thicker films (that is, for low draw ratios), no permanent molecular orientation is possible for PP due to fast relaxation (T_{core} is 40°C above T_m of PP). For the more highly drawn films, film thickness takes values between 0.2 and 0.25 mm. Core temperatures of those films are still high (around 180°C), whereas skin temperatures are expected to be closer to the melting temperature of PP. A competition between orientation and relaxation may therefore be expected at the surface of the highly drawn films.

Depending on the grade of the PP matrix and irrespective of the kind of mixing (one or two steps), two general behaviours were observed. For the PPhv matrix, large surface defects were observed on the extruded film and it was not possible to reach draw ratios higher than 3. Above this value, PP/EVOH films tend to craze. For the PPlv matrix, no surface defects were observed and it was possible to reach draw ratio values as high as 10.

For PP/EVOH blends with 10 vol.% EVOH, the dominant structure induced by the drawing is fibrillar for EVOH [see *Figure 3a–c*]. Fibril diameters decrease as the draw ratio increases. Films with draw ratios larger than 2.5 presented only a fibrillar structure. No breakup and relaxation of EVOH filament back to spherical particles was observed. This may be explained using theories of shape relaxation[35]. When the minor phase is being deformed under elongational flow, there is a competition between the extensional flow that tends to stretch particles into fibres and the shape relaxation. The stretching of particles (diameter a) is the dominant phenomenon when

$$|(da/dt)_{elongation}| > |(da/dt)_{relaxation}| \quad (4)$$

$(da/dt)_{elongation}$ is the average diameter reduction rate due to elongation, whereas $(da/dt)_{relaxation}$ is the average diameter reduction rate due to Rayleigh instability. For sake of simplicity, let us assume a constant macroscopic strain rate $\dot{\epsilon}$. One obtains $\dot{\epsilon} = \ln(\lambda)/\Delta t$. λ is the draw ratio ($\lambda = v_{rolls}/v_{extrusion}$) and Δt the time of stretching. Since elongation occurs within the first $L_0 = 5$ cm from the die, one obtains $\Delta t = L_0/v_{rolls}$. Assuming that the deformation of particles is homothetic of the film deformation and that the drawing is approximately uniaxial, we acquire

$$|1/a_0(da/dt)_{elongation}| = (v_{rolls}/2L_0)\ln(v_{rolls}/v_{extrusion}) \quad (5)$$

where a_0 is the initial radial dimension of the particle, $v_{extrusion}$ is the extrusion speed and v_{rolls} is the linear speed

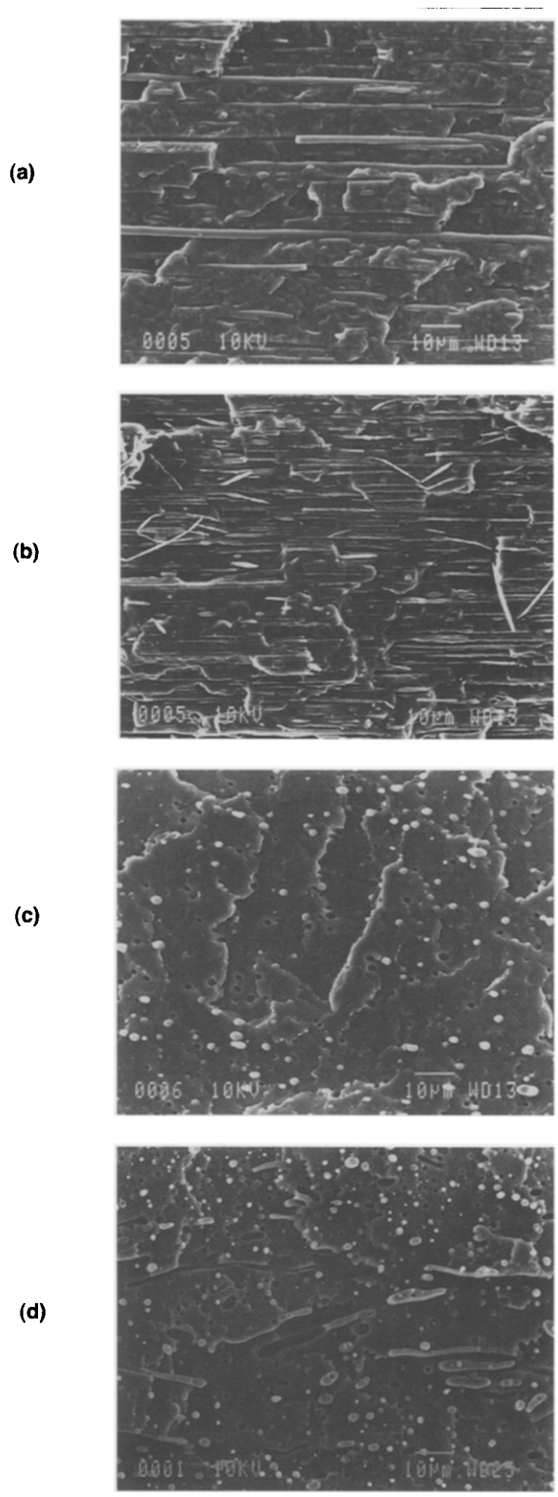

Figure 3 SEM micrograph for PP/EVOH extruded film at different draw ratio λ. Micrographs are taken along the drawing (machine) direction (MD) or transversely to the machine direction (TD): (a) PPlv/(PP.g.MA-EVOH) 80/(10-10) extruded film, λ = 2.8, along MD; (b) PPlv/(PP.g.MA-EVOH) 80/(10-10), λ = 8.7, along MD; (c) PPlv/(PP.g.NM-EVOH) 80/(10-10) extruded film, λ = 2.8, along TD; (d) PPlv/(PP.g.MA-EVOH) 60/(20-20), λ = 3.2, along TD

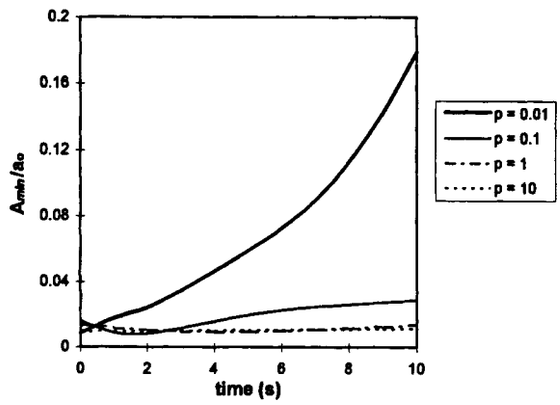

Figure 4 A_{min}/a_0 *versus* time for different viscosity ratios p

Figure 4 for a viscosity ratio, p, ranging from 0.01 to 10. It is then possible, from the slope of curves of $A_{min}/a_0 = f(t)$, to evaluate $(1/a_0(da/dt)_{relaxation})$. $(1/a_0(da/dt)_{elongation})$ and $(1/a_0(da/dt)_{relaxation})$ values are presented in *Table 5*. For draw ratios of 3 and 10, and viscosity ratios between 0.01 and 10, the relaxation rate is always lower than the stretching rate. Therefore, there must be formation of fibrils in the first 5 cm from the exit of the die where stretching occurs.

Once the fibrils are formed, fibrils shape relaxation may still occur in the film section where no stretching occurs. Five centimetres from the die up to the rolls, the film width remains constant, indicating that no stretching occurs there. The maximum time during which fibrils had chance to relax is given by $t = L/v_{rolls}$, where L is the distance between the die (200°C) and the cold rolls (25°C), and v_{rolls} is the linear

Table 5 Elongation and relaxation rates for different draw ratios

V_{rolls} (m s^{-1})	Draw ratio	$1/a_0\,(da/dt)_{elongation}$ (s^{-1})	Viscosity ratio	Drawing time (s)	$1/a_0\,(da/dt)_{elongation}$ (s^{-1})
0.03	2.8	0.3	0.01–0.1	1.7	0.0–0.01
		0.1–10	0.0–0.002		
0.10	8.7	2.2	0.01–0.1	0.5	0.0–0.01
			0.1–10		0.0–0.002

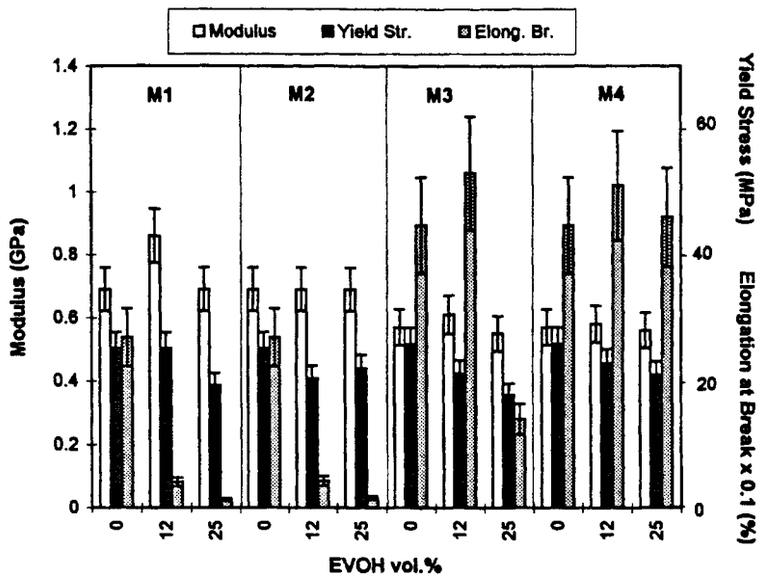

Figure 5 Modulus (▨), yield stress (■) and elongation at break (□) *versus* EVOH concentration for PP/EVOH systems blended on the batch mixer: (M1) PPhv/EVOH, 200°C, 38 rpm; (M2) PPhv/EVOH, 230°C, 38 rpm; (M3) PPIY/EVOH, 200°C, 30 rpm; (M4) PPIv/EVOH, 200°C, 60 rpm

of the rolls. $(da/dt)_{relaxation}$ may be estimated in the following way. When relaxation occurs, the diameter of the fibre at the necking $a_{relaxation}$ is given by

$$a_{relaxation} = a_0 - A_{min} \tag{6}$$

where A_{min} is the depth of the necking on the fibril when shape relaxation occurs and a_0 is the radius of the fibril before relaxation. A_{min}/a_0 with respect to time has been computed for a mixture of two immiscible Newtonian fluids by Tjahjadi *et al.*[36]. Levitt *et al.*[37] have shown that Tjahjadi *et al.*'s[36] calculations give a proper account of behaviours observed for immiscible non-Newtonian polymer blends such as polypropylene–polystyrene. We therefore used Tjahjadi *et al.*'s calculations to estimate A_{min}/a_0 with respect to time for different viscosity ratios. Results are presented in

speed of the rolls. The value of L is approximately 30 cm. At a draw ratio of 3, $v_{rolls} = 0.03$ m s^{-1} leading to $t = 10$ s, and for a draw ratio of 10, $v_{rolls} = 0.10$ m s^{-1} leading to $t = 3$ s. For viscosity ratios ranging from 0.01 to 10, A_{min}/a_0 takes values between 0.01 and 0.12 (see *Figure 4*). When the viscosity ratio increases, A_{min}/a_0 decreases to 0. This means that no filament breakup is possible for viscosity ratios larger than 0.01 at $t = 10$ s. Low amplitude oscillatory shear measurements at frequencies ranging from 0.01 to 100 s^{-1} showed that η_{EVOH}/η_{PP} varies from 0.1 to above 10 for the different PP grade. If the Cox–Merz rule holds then

$$\left[\eta^*_{EVOH}/\eta^*_{PP}\right]_{oscill} = \left[\eta_{EVOH}/\eta_{PP}\right]_{extruder} \tag{7}$$

It follows that $(\eta_{EVOH}/\eta_{PP})_{extruder}$ larger than 0.1. Tjahjadi *et*

al.'s calculations therefore explain why no shape relaxation and fibrils breakup were observed for our blends.

When EVOH concentration is 20 vol.%, two kinds of structure coexist: fibrils together with lamellae of EVOH [see *Figure 3d*]. This is true for PP/EVOH, PP/(PP.g.MA-EVOH) as well as PP/(HDPE-EVOH). Lamellae are probably the results of coalescence between fibrils.

In the case of HDPE/EVOH blends, there appears to be a narrow composition range (from 40 to 50 vol.% EVOH) within which blends exhibit an interpenetrated network-like structure.

Mechanical properties

Data concerning stress at break are not reported here since their evolution with respect to blends composition or draw ratio was found to be similar to that of yield stress. On average, stress at break values were found to be 15% higher than the corresponding yield stress values.

The results concerning the blends prepared on the internal mixer (modulus, yield stress σ_y and elongation at break ϵ_b for pure polymers as well as for PP/EVOH blends) are presented in *Figure 5*. Within experimental uncertainty, moduli are not affected by the addition of EVOH up to 25 vol.%. There is a general decrease in σ_y and ϵ_b when concentration is increased. The decrease of σ_y may be due to debonding between PP and EVOH and haze apparition at the PP–EVOH interface. The large decrease in ϵ_b in the case of PPhv/EVOH may be explained by the presence of large EVOH particles in the PPhv matrix (see the later section on morphology). Large EVOH particles interrupt the PP polymer network and cause breakage at small strain.

The results concerning the samples drawn between rolls after extrusion are presented in *Figures 6* and *7*. Samples containing EVOH with 10 vol.% exhibit very similar mechanical properties to those of the PP matrix extruded and drawn under the same conditions (*Figure 6*). Moreover, at draw ratios below 3, the extruded films have properties similar to those obtained after hot pressing of granules. This confirms that PP films do not show any macromolecular orientation after extrusion and drawing at 200°C at low draw ratio. For the highest draw ratio ($\lambda = 8.7$), a slight increase in modulus is obtained. This may be attributed to low

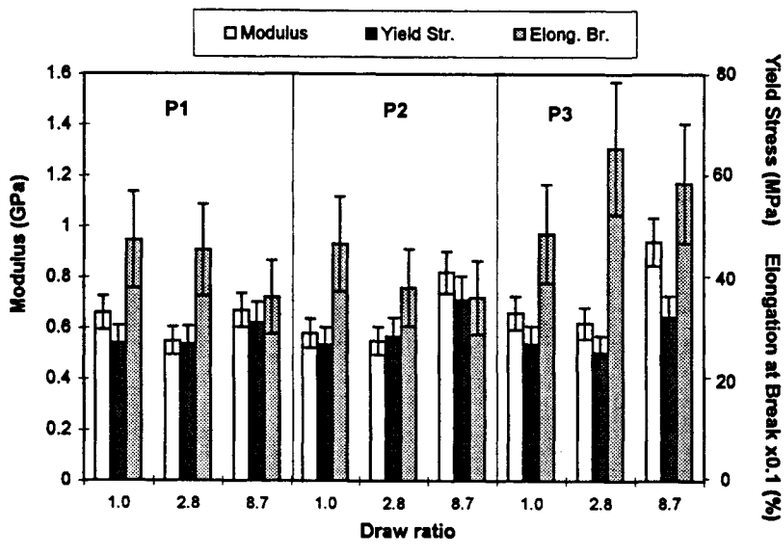

Figure 6 Modulus (▨), yield stress (■) and elongation at break (□) *versus* draw ratio for extruded systems containing 10 vol.% EVOH: (P1) PPlv; (P2) PPlv/EVOH; (P3) PPlv/(PP.g.MA-EVOH)

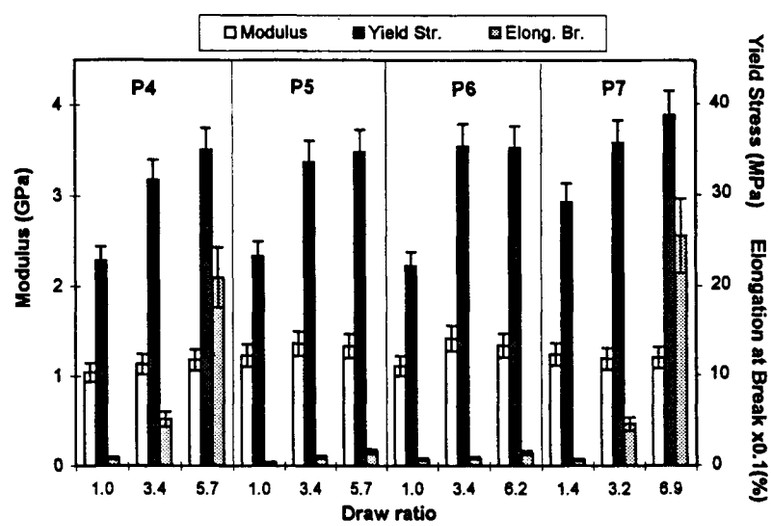

Figure 7 Modulus (▨), yield stress (■) and elongation at break (□) *versus* draw ratio for extruded systems containing 20 vol.% EVOH: (P4) PPlv/(HDPE-EVOH) 60/(2020); (P5) PPlv/(HDPE-EVOH) 50/(30-20); (P6) PPlv/EVOH 80/20; (P7) PPlv/(PP.g.MA-EVOH) 60/(20-20)

Table 6 Lap shear tests data

Sample	Stress at break (MPa)	Elongation at break (%)
PPlv > < EVOH	6.6 ± 0.5	2.1 ± 0.3
PP.g.MA > < EVOH	6.4 ± 2.5	5.6 ± 1.2

Barrier properties of PP-EVOH blends

Barrier properties of multi-layers structure. The permeability to oxygen P_{O_2} measured for PPlv/EVOH/PPlv films is 1.1 $cm^3\ mm^{-1}/(m^2\ day^{-1}\ atm^{-1})$. When compared to PPlv permeability [70.9 $cm^3\ mm^{-1}/(m^2\ day^{-1}\ atm^{-1})$],

Table 7 Barrier properties of PP/EVOH systems blended on the batch mixer

Sample	Vol.%	T_{mixing} (°C)	Ω (rpm)	Measured P_{O_2} [mm $cm^{-3}/(m^2\ day^{-1}\ atm^{-1})$]	P_{O_2} (Maxwell) [mm $cm^{-3}/(m^2\ day^{-1}\ atm^{-1})$]
PPlv				70.9	
PPhv				64.3	
EVOH				0.09	
PP1v/EVOH	83.5/12.5	200	30	81.7	59.1
	83.5/12.5	200	60	58.1	59.1
	75/25	200	30	69.9	47.7
	75/25	200	60	65.6	47.7
	83.5/12.5	200	200	59.9	53.6
PPhv/EVOH	83.5/12.5	200	200	75.0	53.6
	83.5/12.5	230	230	63.9	53.6
	75/25	200	200	233.0	43.3
	75/25	200	200	109.2	43.3
	75/25	230	230	73.5	43.3

macromolecular orientation and also to the fibrillar structure of the drawn blends.

In the case of samples containing 20 vol.% EVOH, the modulus takes a value of about 1.2 GPa, irrespective of the process (*Figure 7*). Only a slight increase is observed with the draw ratio. This value is 50% above the measured modulus of the matrix. This is to be expected at 20 vol.% EVOH since the modulus of EVOH is more than 3.5 times higher than that of PP. σ_y values are more sensitive to the draw ratio than to the preparation method of the blends. There is a general increase of σ_y with the draw ratio. This significant increase of σ_y may be attributed to the apparition of a large fibrils fraction (twice as much as for PPlv/EVOH blends with 10 vol.% EVOH) when drawing occurs. ϵ_b depends on the processing conditions as well as on the draw ratio. In the case of samples containing PP and EVOH but no HDPE, the rupture of the sample occurs at low elongation value when no compatibilizer is added. When PP.g.MA is added, the larger the draw ratio, the larger the value of ϵ_b. For the largest draw ratio ($\lambda = 6$), ϵ_b takes a value of 250%. Without PP.g.MA, this value is more than 10 times lower.

In the case of the PPlv/(HDPE-EVOH) blends, ϵ_b decreases when the HDPE concentration increases. When the minor phases concentration is 40 vol.%, ϵ_b increases sharply with the draw ratio, in the same way as for PPlv/(PP.g.MA-EVOH). This may be due to the great ductility of HDPE, with ϵ_b up to 800%. However, a slight increase in the minor phase concentration (from 40 to 50 vol.%) induces a sharp fall in ϵ_b for draw ratios above 1. This 50 vol.% EVOH may be in that case a threshold value above which the PP macromelecular network is interrupted whatever the morphology.

Results concerning the lap shear tests are presented in *Table 6*. Although stress at break are similar for PPlv stuck to EVOH and PP.g.MA stuck to EVOH, elongation at break is larger for the last set of samples, indicating that PP.g.MA adheres to EVOH even at larger strains. This means that adhesion between PP and EVOH is enhanced by the MA groups bonding chemically EVOH chains to PP chains.

permeability results clearly show that high barrier properties can be achieved by mixing PP and EVOH as long as a way to flatten EVOH particles is found. Experimental data have also been compared to permeability given by the series model for which

$$1/P = \phi^{PP}/P^{PP} + \phi^{EVOH}/P^{EVOH} \quad (8)$$

where ϕ^{PP} (ϕ^{EVOH}) is the volume fraction of the PP (EVOH) phase and P^{PP} (P^{EVOH}) is the permeability of the PP (EVOH) phase. P^{EVOH} value was found to be 0.09 $cm^3\ mm^{-1}/(m^2\ day^{-1}\ atm^{-1})$. In the case of multi-layer films, ϕ^{EVOH} is simply given by

$$\phi^{EVOH} = (\text{EVOH layer thickness})/(\text{total film thickness}) \quad (9)$$

Average thicknesses of layers were measured after permeability tests by removing each layer from the other. This was easy in the case of the PPlv/EVOH/PPlv due to the poor adhesion between PP and EVOH. The series model value($\{P_{O_2}^{Model} = 1.0\ cm^3\ mm^{-1}/(m^2\ day^{-1}\ atm^{-1})$ fits well experimental values of P_{O_2}.

Dispersed morphology (batch blending). The pertneabilities determined for the pure polymers and blends are given in *Table 7*. Values corresponding to pure polymers fit well those given in the literature for poorly oriented PP (cf. Taraiya *et al.*[38]) and EVOH (cf. Culter[26]).

For the PPlv matrix, blends permeabilities to O_2 range from 58 to 80 $cm^3\ mm^{-1}/(m^2\ day^{-1}\ atm^{-1})$ with no correlation to EVOH concentration (from 12 to 25 vol.%), rotor speed (from 30 to 60 rpm). Only a slight decrease in permeability is observed as compared to the PPlv alone. For the PPhv matrix, permeability to O_2 ranges from 65 to 230 $cm^3\ mm^{-1}/(m^2\ day^{-1}\ atm^{-1})$ with no correlation to EVOH concentration (from 12 to 25 vol.%), rotor speed (from 30 to 60 rpm) and mixing temperature (from 200 to 230°C). Scattered permeability results may be explained by two conflicting effects:

- EVOH particles tend to decrease permeability;

- due to the poor adhesion between PP and EVOH, voids may appear at the interface, increasing the permeability.-Morphological analyses show that in the case of a PPhv matrix, the mixing is very inhomogeneous. For large EVOH concentration (25 vol.%), the interface between EVOH particles and the PP matrix can run from one side of the film to the other. Voids can then run from one side to the other, increasing the permeability values to levels higher than the permeability value of the PP alone. For lower EVOH content (12 vol.%), no such large EVOH particles exist and permeabilities are lower.

In the case of PPlv-EVOH films, EVOH particles dispersion is better (no PP–EVOH interface running from one face of the film to the other) and voids level seems lower. Blends permeabilities are on average slightly smaller than the PPlv permeability.

In the Maxwell model considering spherical particles of permeability P_d embedded in a matrix of permeability P_m, the permeability P of the blend is given by[15]

$$P = P_m(P_d + 2P_m - 2\phi_d(P_m - P_d))/(P_d + 2P_m + \phi_d(P_m - P_d)) \quad (10)$$

For most of our samples, measured permeabilities are generally higher than those predicted by the Maxwell model. Discrepancy with the model predictions may be attributed to the presence of voids in the blends.

Fibrillar morphology (continuous blending). Results are presented in *Table 8*. For most of the PP/EVOH blends with 10 vol.% EVOH and draw ratios larger than 3, permeabilities take values ranging from 22 to 25 $cm^3\ mm^{-1}/(m^2\ day^{-1}\ atm^{-1})$, irrespective of the kind of mixing used. Those values are 2.5 to 3 times lower than those obtained for the PP matrix alone, although the concentration of EVOH is low (10 vol.%). No significant change in permeability is observed when draw ratio λ is increased from 3 to 9. This is an expected result since the morphology is fibrillar in both cases. Fibrils are thinner at $\lambda = 9$, but distances between fibrils are also smaller. Since morphologies are homothetic from $\lambda = 3$–9, tortuosities should remain similar from $\lambda = 3$–9. With 20 vol.% EVOH, permeabilities are seven times lower than those obtained for the pure PP. In the case of PPlv/(HDPE-EVOH) films with 20 vol.% EVOH, barrier properties are not as good as those for PPlv/EVOH films. This may be due to poor adhesion between PP and HDPE interfaces. This leaves voids in the sample through which O_2 molecules can diffuse. However, barrier properties are still better than for the PPlv matrix alone.

It is interesting to compare these experimental results with diffusion models. The cylindrical model considers cylinders of permeability P_d embedded in a matrix of permeability PM, the permeability P_d of the material is given by (see Appendix A)

$$P = P_m\left(1 + \frac{2\phi_d}{\frac{r+1}{r-1} - \phi_d + 0.3\frac{r-1}{r+1}\phi_d^4 + 0.013\frac{r-1}{r+1}\phi_d^8}\right) \quad (11)$$

ϕ_d is the volume fraction of the dispersed particles and $r = P_d/P_m$. It is worth mentioning that the maximum packing concentration for cylinders is $\phi_d = 0.79$. Above this limit, equation (11) no longer holds. Since in our experiments $r < 1$ and $\phi_d < 0.3$, r can be set at 0 in equation (11) and terms in ϕ_d^4 and ϕ_d^8 can be neglected with respect to ϕ_d. equation (11) can then be approximated by

$$P = P_m(1 - \phi_d)/(1 + \phi_d) \quad (12)$$

Experimental values of permeabilities are lower than those predicted by the cylindrical model (see *Table 8*). This discrepancy between the cylindrical model and experiment may be expected. EVOH fibrils are randomly dispersed in the plane perpendicular to the draw direction. However, in the cylindrical model, fibres are supposed to be regularly aligned at equal distance from each other. In the cylindrical model, O_2 molecules can diffuse straight across the PP matrix, without crossing an EVOH fibre on their path. In the case of a random distribution of the fibres in the film cross-section, O_2 molecules have to bypass the EVOH fibres. This significantly increases the diffusion time of O_2 molecules through the film thickness and therefore decreases the permeability. At 20 vol.% EVOH, lamellae are also present. Since EVOH lamellae increase much more the path of O_2 molecules through the PP matrix than fibrils, this gives another reason for permeability to be lower than that predicted by the cylindrical model.

Some of the PP/EVOH blends exhibit a hybrid structure with both EVOH lamellae and EVOH fibrils. An hybrid diffusion model combining the series model and the cylindrical model is therefore proposed. In this model, the

Table 8 Barrier properties of PP/EVOH extruded films

Sample	Vol.%	Draw ratio	Permeability [mm $cm^{-3}/(m^2\ day^{-1}\ atm^{-1})$]			Series fraction ϕ_s (%)
			Measured	Cylindrical	Series	
PPhv			64.3			
PPlv			70.9			
EVOH			0.09			
PPhv/(PP1v-EVOH)	80/(10-10)	3.4	22.4	53.2	1.1	59.8
PPlv/EVOH	90/10	2.8	22.1	58.0	1.1	64.3
	80/20	3.4	12.4	47.3	2.2	75.5
PPlv/PP.g.MA/EVOH	80/10/10	2.8	23.1	62.5	1.1	62.5
	80/10/10	8.7	25.5	62.5	1.1	58.2
PPlv/(PP.g.MA-EVOH)	80/(10-10)	2.8	30.1	62.5	1.1	50.0
	80/(10-10)	8.7	25.0	62.5	1.1	59.1
	60/(20-20)	3.2	9.5	37.5	2.2	81.8
PPLv/(HDPE-EVOH)	60/(20-20)	3.4	51.6	52.1	2.2	

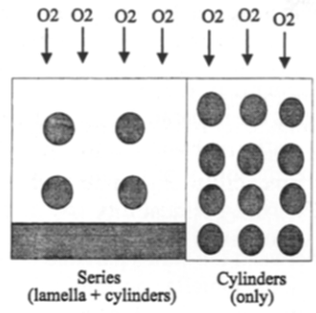

Figure 8 Schematic of the hybrid model

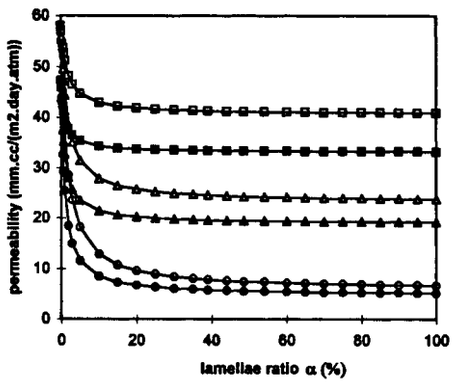

Figure 9 Hybrid model permeability *versus* lamellae ratio a for different series fraction ϕ_d: (○) $\phi_s = 0.9$ and $\phi_d = 0.1$; (●) $\phi_s = 0.9$ and $\phi_d = 0.2$; (△) $\phi_s = 0.6$ and $\phi_d = 0.1$; (▲) $\phi_s = 0.6$ and $\phi_d = 0.2$; (▨) $\phi_s = 0.3$ and $\phi_d = 0.1$; (■) $\phi_s = 0.3$ and $\phi_d = 0.2$

material is conceptually divided in two parts in parallel. One part has minor phase cylinders (EVOH fibrils) embedded in the matrix (PP). The other part has one lamella in parallel with cylinders (see *Figure 8*). The minor phase concentrations are supposed to be the same for both parts. Two parameters control the morphology, ϕ_s is the volume fraction of the series part. This parameter controls the lamella surface. When ϕ_s is equal to 1, the lamella covers the whole surface of the sample. α is the ratio of the lamellae volume to the minor phase volume in the series part. α controls the thickness of the lamella. The larger the value of α, the thicker are the lamellae. The hybrid model gives for the permeability of the blend the following result:

$$P = \frac{\phi_s}{\dfrac{\alpha\phi_d}{P_d} + \dfrac{(1-\alpha\phi_d)(1-2\alpha+\phi_d)}{P_m(1-2\alpha)(1-\phi_d)}} + \frac{(1-\phi_s)(1-\phi_d)P_m}{1+\phi_d} \tag{13}$$

Details of the calculations are given in Appendix B. As shown in *Figure 9*, when the lamellae ratio α is higher than 40%, permeability remains constant for a given ϕ_s. To limit the number of variables in equation (13), it is then convenient to set α at a given value. Experimentally, only a few lamellae are present at 10 and 20 vol.% EVOH. α was therefore set at the minimum value above which P only depends on ϕ_s (i.e. $\alpha = 40\%$). The volume fraction of lamellae ϕ_L is given by

$$\phi_L = \phi_s\phi_d\alpha \tag{14}$$

ϕ_L can be experimentally measured from image analysis of SEM micrographs. It may also be determined from the approach used by Levit *et al.*[37]

The hybrid model give series fraction, ϕ_s, ranging from 50 to 64% at 10 vol.% EVOH (see *Table 8*). From equation (14), the equivalent lamellae fraction ϕ_L range from 2 to 2.5%. This shows that blends with 10 vol.% EVOH are behaving as if a small amount of lamellae were present. However, the experimental value of ϕ_L should be 0% since no lamellae can be detected at 10 vol.% EVOH. At 20 vol.% EVOH, the series fraction ϕ_s takes values between 75 and 82% (see *Table 8*) and the corresponding lamellae fraction ϕ_L is around 8 vol.%. This is three to four times the theoretical lamellae fraction at 20 vol.% EVOH. This accounts semi-quantitatively for the presence of lamellae. At 20 vol.% EVOH, experimental valueof ϕ_L is around 5% [see *Figure 3*(d)].

Measured permeabilities are of course larger than those predicted by the series model (lamellae of EVOH parallel to the film plane). In our case, the morphology is clearly mainly fibrillar at 10 vol.% EVOH, and even at 20 vol.% EVOH there is still a large proportion of fibrils [see *Figure 3*(d)]. As already stated by Gopalakrishnan *et al.*[19] in case of PET/EVOH blends, the most important factor leading to improved barrier properties is the obtention of an oriented morphology, irrespective of the use of a compatibilizer.

CONCLUSION

Morphology, thermal, mechanical and barrier properties of PP/EVOH, PP/(PP.g.MA-EVOH) and PP/(HDPE-EVOH) blends have been studied. It has been shown that high increase in barrier properties of PP can be obtained by adding only small amounts of EVOH. Barrier properties of the blends are mainly controlled by EVOH concentration and EVOH particles morphology, irrespective of the processing conditions. The key condition for high barrier properties is the obtention of an oriented morphology. When the aspect ratio of EVOH particles is low, decrease in permeability was small (less than 15 vol.%) for EVOH concentration ranging from 12 to 25 vol.%. In the case of extrusion and drawing process, for blends containing 20 vol.% EVOH, lamellae appear together with fibrils. Permeabilities are as much as seven times lower than for pure PP. This is a significant increase in barrier properties as compared to results obtained so far. This increase in barrier properties is properly taken into account by an hybrid permeability model. The fitting parameter introduced to account for the morphology of the blend can be obtained either from image analysis of SEM-micrographs or using Levitt *et al.*'s approach[37]. When compared to PP/EVOH extruded and drawn blends, PP/(HDPE-EVOH) blends exhibit poor barrier properties, probably due to void formation along the interfaces between the phases.

Mechanical properties of the PPlv/EVOH films are very similar to that of the pure PP when EVOH concentration is 10 vol.%. When PP.g.MA is added to PPlv/EVOH blends containing 20 vol.% EVOH, elongation at break remains important. This result, together with the high increase in barrier properties, makes the PPlv/(PP.g.MA-EVOH) material with 20 vol.% EVOH suitable for applications such as packaging or pipeing. The low-cost matrix and the low processing cost make the final material very competitive for the food packaging market.

ACKNOWLEDGEMENTS

The authors acknowledge the financial support provided by the NSERC (Natural Sciences and Engineering Research Council of Canada) and the FCAR (Fonds pour la Formation de Chercheurs et l'Aide à la Recherche du Québec). Himont

Canada, EVAL Co. of America, Novacor–Canada and Mitsubishi Chemical Co. of Japan are gratefully acknowledged for providing polymer samples.

APPENDIX A:

Sax and Ottino[39] have shown that the coefficient of diffusion through a medium containing cylinders of diffusion coefficient D_d randomly oriented in a continuous medium of diffusion coefficient D_m is given by [see equations (30) and (32) of Ref. [39]]:

$$D_{eff} = \frac{D_{11} + D_{22} + D_{33}}{3} \tag{A1}$$

D_{33} is the diffusion coefficient for the diffusion parallel to the cylinder axis (axial diffusion):

$$D_{33} = \frac{D_m A_{ax}}{s\left(1 + \phi_c \dfrac{(1-s)}{s}\right)} \tag{A2}$$

with

$$A_{ax} = 1 - \phi_d + \phi_d x s \tag{A3}$$

ϕ_d is the dispersed phase concentration, x is the diffusively ratio (D_d/D_m) and s is the solubility ratio (S_d/S_m).

D_{11} and D_{22} are the diffusion coefficients for the diffusion along two directions perpendicular to one another and to the cylinder axis (radial diffusion):

$$D_{11} = D_{22} = \frac{D_m A_{rad}}{s\left(1 + \phi_c \dfrac{(1-s)}{s}\right)} \tag{A4}$$

with

$$A_{rad} = 1 + \frac{2\phi_d}{\dfrac{sx+1}{sx-1} - \phi_d + 0.3\dfrac{sx-1}{sx+1}\phi_d^4 + 0.013\dfrac{sx-1}{sx+1}\phi_d^8} \tag{A5}$$

The effective solubility is given by

$$S_{eff} = \phi_m S_m + \phi_d S_d \tag{A6}$$

Since $s = S_d/S_m$ and $\phi_d = 1 - \phi_m$, the following relation holds:

$$S_{eff} = S_m s(1 + \phi_m(1-s)/s) \tag{A7}$$

Multiplying equation (A.1) by S_{eff} and using equation (A.7) leads to

$$S_{eff} D_{eff} = S_m D_m (A_{ax} + 2A_{rad})/3 \tag{A8}$$

Since the effective permeability of the medium is by definition $P_{eff} = S_{eff} D_{eff}$, this leads to

$$P_{eff} = (P_{ax} + 2P_{rad})/3 \tag{A9}$$

with $P_{ax} = P_m A_{ax}$ and $P_{rad} = P_m A_{rad}$.

Equation (A.9) gives the permeability for a material containing randomly oriented cylinders of permeability $P_d = S_d D_d$ in a continuous medium of permeability $P_m = S_m D_m$. However, in our case, the diffusion is only radial since all EVOH fibres are oriented perpendicularly to the direction of O_2 diffusion. Therefore, the permeability of a material with cylinders (permeability P_d) perpendicular to the direction of diffusion is P_{rad}. This can be written as

$$P_{rad} = P_m \left[1 + \frac{2\phi_d}{\dfrac{r+1}{r-1} - \phi_d + 0.3\dfrac{r-1}{r+1}\phi_d^4 + 0.013\dfrac{r-1}{r+1}\phi_d^8}\right] \tag{A10}$$

with $r = sx = P_d/P_m$.

APPENDIX B: PERMEABILITY FROM THE HYBRID MODEL

A conceptual schematic of the hybrid model is presented on *Figure 8*. Two parts are in parallel, one with one lamella and cylinders (series part), and one with cylinders only (cylinders part). The permeability of the material is given by

$$P = \phi_s P_s + (1 - \phi_s) P_c \tag{B1}$$

The difference between the series part and the cylinders part is the following: some lamellae appear in the series part due to coalescence between fibrils, whereas in the cylinders part, no coalescence occurs. However, this difference in morphology does not imply any difference in dispersed phase concentration since lamellae are fibrils stuck together. It therefore seems reasonable to make the simple assumption that the dispersed phase fraction is the same in the series part (ϕ_{ds}) and the cylinders part (ϕ_{dc}):

$$\phi_d = \phi_{ds}\phi_{dc} \tag{B2}$$

Permeability of the cylinders part is therefore given by

$$P_c = P_m(1 - \phi_d)/(1 + \phi_d) \tag{B3}$$

Permeability of the series part is given by

$$\frac{1}{P} = \frac{\phi_{LS}}{P_d} + \frac{1 - \phi_{LS}}{\dfrac{1 - \phi_{CS}}{1 + \phi_{CS}} P_m} \tag{B4}$$

where ϕ_{LS} is the lamellae fraction in the series part and ϕ_{CS} is the cylinder fraction. It is easy to show that

$$\phi_{LS} = \alpha\phi_d \tag{B5}$$

α is the ratio of the lamellae volume to the dispersed phase volume in the series part, and ϕ_{CS} is given by

$$\phi_{CS} = (1 - \alpha)\phi_d/(1 - 2\alpha + \alpha\phi_d) \tag{B6}$$

Therefore, the permeability of the blend is given by

$$P = \frac{\phi_s}{\dfrac{\alpha\phi_d}{P_d} + \dfrac{(1 - \alpha\phi_d)(1 - 2\alpha + \phi_d)}{P_m(1 - 2\alpha)(1 - \phi_d)}} + \frac{(1 - \phi_s)(1 - \phi_d)P_m}{1 + \phi_d} \tag{B7}$$

REFERENCES

1. Leaversuch, R.D., *Modern Plastics*, 1994, **July**, 48.
2. Lindsay, K.F., *Modern Plastics*, 1992, **January**, 104.
3. Mapleston, P., *Modern Plastics*, 1992, **June**, 62.
4. Bonis, L. J., in *Plastic Film Technology, High Barrier Plastic Films for Packaging*, Vol. 1. Technomic, Lancaster, PA, 1989, p. 80.
5. Salame, M., in *Plastic Film Technology, High Barrier Plastic Films for Packaging*, Vol. 1. Technomic, Lancaster, PA, 1989, p. 132.
6. Bourque, R. A., in *Plastic Film Technology, High Barrier Plastic Films for Packaging*, Vol. 1. Technomic, Lancaster, PA, 1989, p. 32.
7. Jabarin, S.A. and Kollen, W.J., *Polymer Engineering Science*, 1988, **28**, 1156.
8. Schreiber, P., *Plastics Engineering*, 1986, **May**, 26.
9. Brahimi, B., Aït-Kadi, A., Ajji, A., Fayt, R. and Pol, J., *Science: Part B: Polymer Physics*, 1991, **29**, 945.
10. Bousmina, M. and Muller, R., *Rheologica Acta*, 1996, **35**, 369.
11. Ikari, K. and Moritani, M., in *Proceedings, COEX '84*. Princeton, NJ, Schotland Business Research, Inc, 1984, p. 289.
12. Subramanian, P.M., *Polymer Engineering Science*, 1985, **25**, 483.
13. Subramanian, P.M. and Mehra, V., *Polymer Engineering Science*, 1985, **25**, 663.
14. Lee, S.-Y. and Kim, S.-C., *International Polymer Processing*, 1996, **3**, 238.
15. Lohfink, G.W. and Kamal, M.R., *Polymer Engineering Science*, 1993, **33**, 404.

16. Grace, H.P., *Chemical Engineering Communications*, 1982, **14**, 225.
17. Kamal, M.R., Garmabi, H., Hozhabr, S. and Arghyris, L., *Polymer Engineering Science*, 1995, **35**, 41.
18. Gaylord, N. G., Ender, H. and David, L. R., in: *Proceedings of the 52th Annual Conference, ANTEC-94*. 1994, Part 2, p. 1646.
19. Gopalakrishnan, R., Schultz, J.M. and Gohil, R., *Journal of Applied Polymer Science*, 1995, **56**, 1749.
20. Kit, K.M., Schultz, J.M. and Gohil, R., *Journal of Polymer Engineering Science*, 1995, **35**, 680.
21. McCormack, T., *Modern Plastics*, 1993, **April**, 77.
22. Technical Information of EVAL EP-F Series, EVAL Co. of America, 1995.
23. Leaversuch, R.D., *Modern Plastics*, 1994, **October**, 22.
24. Technical Information of Himont Profax resins, Himont, Canada, 1995.
25. Blackwell, A. L., in *Plastic Film Technology, High Barrier Plastic Films for Packaging*, Vol. 1. Technomic, Lancaster, PA, 1989, p. 41.
26. Culter, J. D., *High Barrier Plastic Films for Packaging*, Vol. 1. Technomic, Lancaster, 1989, p. 32.
27. Technical Information of Novapol resins, Novacor, Canada, 1995.
28. Mirabella, F.M., *Journal of Polymer Science Part B*, 1987, **25**, 591.
29. Hwang, K.S., Lin, C.A. and Lin, C.H., *Journal of Applied Polymer Science*, 1994, **52**, 181.
30. Modern Controls Inc., Operating manual for the OX-TRAN 10150 oxygen permeability tester, Elk River, MN, 1983.
31. Goodrich, J.E. and Porter, R.S., *Polymer Engineering Science*, 1967, **7**, 1.
32. Faisant, J.B., Bousmina, M. and Ait-Kadi, A., in preparation.
33. Grace, H.P., *Chemical Engineering Communications*, 1982, **14**, 225.
34. Agassant, J.-F., Avenas, P., Sergent, J.-Ph. and Carreau, P. J., *Polymer Processing: Principles and Modeling*. Hanser, 1991.
35. Huneault, M. A., Champagne, M. F. and Luciani, A., in *Proceedings of PolyBlends-95 Symposium*, ed. by L.A. Utracki, 1995, p. 257.
36. Tjahjadi, M., Ottino, J.M. and Stone, H.A., *AIChE Journal*, 1994, **40**, 385.
37. Levitt, L., Macosko., C. W. and Pearson, S. D., in *Proceedings of the PolyBlends-95 Symposium*, ed. by L.A. Utracki L.A., 1995, p. 325.
38. Taraiya, A.K., Orchard, A.J. and Ward, I.M., *Journal of Applied Polymer Science*, 1990, **41**, 1659.
39. Sax, J. and Ottino, J.M., *Polymer Engineering Science*, 1983, **13**, 165.